Journal of Nuclear Materials 493 (2017) 264–270

Contents lists available at ScienceDirect

Journal of Nuclear Materials

journal homepage: www.elsevier.com/locate/jnucmat

Onset conditions for flash sintering of UO_2

Alicia M. Raftery [a, *], João Gustavo Pereira da Silva [b], Darrin D. Byler [a], David A. Andersson [a], Blas P. Uberuaga [a], Christopher R. Stanek [a], Kenneth J. McClellan [a, **]

[a] Los Alamos National Laboratory, Los Alamos, NM 87544, USA
[b] Technical University of Hamburg, Hamburg, Germany

ARTICLE INFO

Article history:
Received 7 March 2017
Received in revised form
16 June 2017
Accepted 16 June 2017
Available online 22 June 2017

Keywords:
Flash sintering
Field assisted sintering
Uranium dioxide
Nuclear Fuel

ABSTRACT

In this work, flash sintering was demonstrated on stoichiometric and non-stoichiometric uranium dioxide pellets at temperatures ranging from room temperature (26°C) up to 600°C. The onset conditions for flash sintering were determined for three stoichiometries ($UO_{2.00}$, $UO_{2.08}$, and $UO_{2.16}$) and analyzed against an established thermal runaway model. The presence of excess oxygen was found to enhance the flash sintering onset behavior of uranium dioxide, lowering the field required to flash and shortening the time required for a flash to occur. The results from this study highlight the effect of stoichiometry on the flash sintering behavior of uranium dioxide and will serve as the foundation for future studies on this material.

© 2017 Elsevier B.V. All rights reserved.

1. Introduction

Uranium dioxide is used to power the majority of commercial nuclear reactors, with more than 50 years of experience acting as the foundation for its use as a nuclear fuel. Uranium dioxide has a number of favorable fuel properties, including good corrosion resistance in water and low swelling under irradiation [1]. Thousands of tonnes of uranium dioxide fuel pellets are fabricated each year for use in the world's nuclear reactors [2]. Sintering is one step in the fabrication process where powder compacts are brought to a high temperature to create high-density ceramic fuel pellets. Conventional sintering of pellets typically takes anywhere from 4 to 6 h in a furnace at temperatures as high as 1750°C. There have been numerous attempts to lower the sintering temperature in order to improve the efficiency of fuel production [3], but any improvements made in temperature reduction still require long sintering times [4].

Field assisted sintering (FAS) describes a group of novel sintering methods that use an electric field and/or current in order to provide powder densification. These techniques have proven to produce a higher level of densification in much shorter time periods compared to conventional sintering [5]. The feasibility of using FAS techniques to fabricate nuclear fuel is gaining recognition due to the potential economic benefits and improvements in material properties [6]. Methods like spark plasma sintering [7] and microwave sintering [8] have already demonstrated the ability to sinter uranium dioxide fuel pellets in a shorter time and lower temperature compared to conventional sintering. These new methods may even hold the key to fabricating advanced fuels, including composites. The shorter sintering time and lower temperatures may mitigate reactions between constituents that would otherwise occur during conventional sintering of composite fuels, thus potentially enabling new nuclear fuel material systems [9,10].

Flash sintering is one type of FAS technique that uses an applied electric field/current and temperature to provide densification of materials on very short time scales. The bulk of sintering can occur in a matter of seconds under the application of an increased field and temperature [11]. The characteristic behavior of flash sintering is a current runaway, which occurs sometime after a critical field is applied across a sample. During the runaway, the current increases until reaching a current limit that is pre-defined in the experimental setup. One interesting observation in several systems is the presence of an incubation time before the current runaway occurs. The incubation time is defined as a time before the flash event where the current density remains low and with a very slow evolution [12]. In addition to shorter sintering times, the furnace temperatures required to sinter with flash sintering have been

* Corresponding author.
** Corresponding author.
E-mail addresses: araftery@purdue.edu (A.M. Raftery), kmcclellan@lanl.gov (K.J. McClellan).

http://dx.doi.org/10.1016/j.jnucmat.2017.06.022
0022-3115/© 2017 Elsevier B.V. All rights reserved.

lower than those used in conventional sintering [13–15]. The general trend observed so far is that the critical field required to flash a sample decreases with an increase in temperature [16].

Material behavior during flash sintering has been linked to applied [17] and material [18] parameters, but the underlying mechanisms active during flash sintering have yet to be identified. Current theories describing the potential mechanisms include electromigration [19], self-cleaning at the grain boundaries [20], and joule heating [21]. However, there is now a general agreement that thermal runaway from joule heating is largely responsible for the current runaway, with recent studies showing good agreement between experiment and model [22–24].

The main objective of this study was to demonstrate flash sintering on uranium dioxide, identifying key parameters (critical field, incubation time) dictating the onset of flash sintering according to a variation in stoichiometry. Some experimental results were analyzed against an existing thermal runaway model for comparison and to provide further model validation. The results therefore act as an initial study on flash sintering of uranium dioxide, which will be expanded upon with future optimization of the process in order to enable UO_{2+x} based fuel sintering with controlled microstructure and density.

2. Materials and methods

2.1. Sample preparation

For starting material, depleted uranium dioxide feedstock from AREVA was used, which was manufactured via the integrated dry route (IDR) with an as-received oxygen-to-metal ratio of $UO_{2.16}$. The feedstock was milled for 15 min in a Spex Certiprep 8100 high-energy mill with a single zirconia ball and vial then sieved through a 400 μm mesh sieve. The resulting powder was milled for 5 min with 1.0 wt% ethylene bis-stearamide (EBS) binder before being pressed in a 4.75 mm dual action punch and die at 60 MPa to obtain a green density of 55% theoretical density (TD). The cylindrical pellets were then pre-sintered under an Ar-6% H atmosphere to a density of 10.42 g/cm^3, or approximately 95% TD. This initial density was used to eliminate densification effects and reduce sample-to-sample variability as this study was focused on flash onset conditions rather than sintering conditions. The stoichiometry was set in a Netzsch STA 409 thermogravimetric analyzer (TGA) to starting stoichiometries of $UO_{2.00}$, $UO_{2.08}$, and $UO_{2.16}$ for the flash experiments. The stoichiometry of each sample was controlled by altering the oxygen potentials in the sintering atmosphere within the TGA and continuously measuring the oxygen with sensors. Lastly, the ends of the pellets were painted with platinum paint and baked in a furnace at 200°C for one hour to remove paint thinner impurities, which reduced variability in the sample-electrode interface resistance. The final pellets had a nominal geometry of 4.75 mm in diameter and 5.25 mm in length.

2.2. Experimental setup

The flash sintering setup consisted of a Netzsch 402C dilatometer furnace and a 5A/150V Agilent N5750A DC power supply. The pellets were placed in the dilatometer with two platinum leads in contact with the ends, which were attached to the power supply and used to apply an electric field across the sample (see Fig. 1). A Fluke 87V digital multimeter was placed in series to measure the system resistance before and after the experiment, and a thermocouple was placed near the sample to record the temperature change of the system. These measurements were taken for qualitative purposes, since they did not accurately represent the exact sample temperature or resistance. The experiments were performed under argon flowing at 500 mL/min and purified to less than 1×10^{-10} ppm O_2 in order to eliminate the possibility of oxidation. The maximum current density allowed to flow through each sample was limited to 50 mA/mm^2. When this limit was reached, the power supply was switched off in order to minimize any densification or grain growth effects.

3. Model description

This work uses the thermal runaway model developed by Pereira da Silva et al. [22], in which the flash sintering event is modeled using bifurcation diagrams as a discontinuity on the equilibrium surface of the stable temperatures, caused by the heat balance between Joule heating and the heat losses to the environment:

$$\frac{E^2 e^{-\frac{\Delta E}{k\theta}}}{\Omega_0} - h(\theta - \theta_0) = 0 \tag{1}$$

where E is the electrical field, ΔE is the activation energy for resistivity, k is the Boltzmann constant, θ is the sample temperature, Ω_0 is the pre-exponential constant for resistivity, h is the heat transfer coefficient for convection and θ_0 is the furnace temperature.

For the sake of simplicity, one can plot the stable temperatures as a function of the electrical field in a bifurcation diagram (lower part of Fig. 2). This bifurcation can be understood with the help of Fig. 2. For electric field values lower than E_{C1}, there is only one stable equilibrium point. Reaching exactly E_{C1}, Joule heating makes the peak on the blue curve cross the equilibrium line, creating a pair of stable and meta-stable points. This second point is meta stable, because it is an unstable point if approached from the left-hand side, and stable from the right-hand side.

Right after E_{C1}, there is a triplet of equilibrium points: stable (green), unstable (red), and stable, respectively. Further increase of electrical field up to E_{C2} makes the valley on the blue line cross the equilibrium line, collapsing two equilibrium points together and creating a metastable (green and red) equilibrium on the leftmost point. Electrical fields higher than E_{C2} lead to only one stable equilibrium point.

Fig. 3 details the transition between the critical points E_{C2} and E_3. At E_{C2}, any starting conditions (sample temperature equal to furnace temperature θ_0), will lead to an equilibrium at the meta-stable point. A slight increase on the electrical field will make this stable point disappear, leading to a sudden heating up to the next stable point on the right-hand side. This sudden thermal runaway can be understood as the onset of flash sintering.

4. Results

4.1. Critical field at isothermal temperatures

4.1.1. Model

In order to predict the critical electrical fields that lead to flash sintering, the resistivity of each composition was estimated from the linear portion of the flash sintering experiments at different temperatures using an Arrhenius temperature dependent behavior:

$$\Omega = \Omega_0 e\left(\frac{\Delta E}{k\theta}\right) \tag{2}$$

The results are plotted in Fig. 4, and the measured values for Ω_0 and ΔE are summarized in Table 1. Ω_0 is assumed to be representative of the sample resistivity since the system resistance is small in comparison and the same for all experiments.

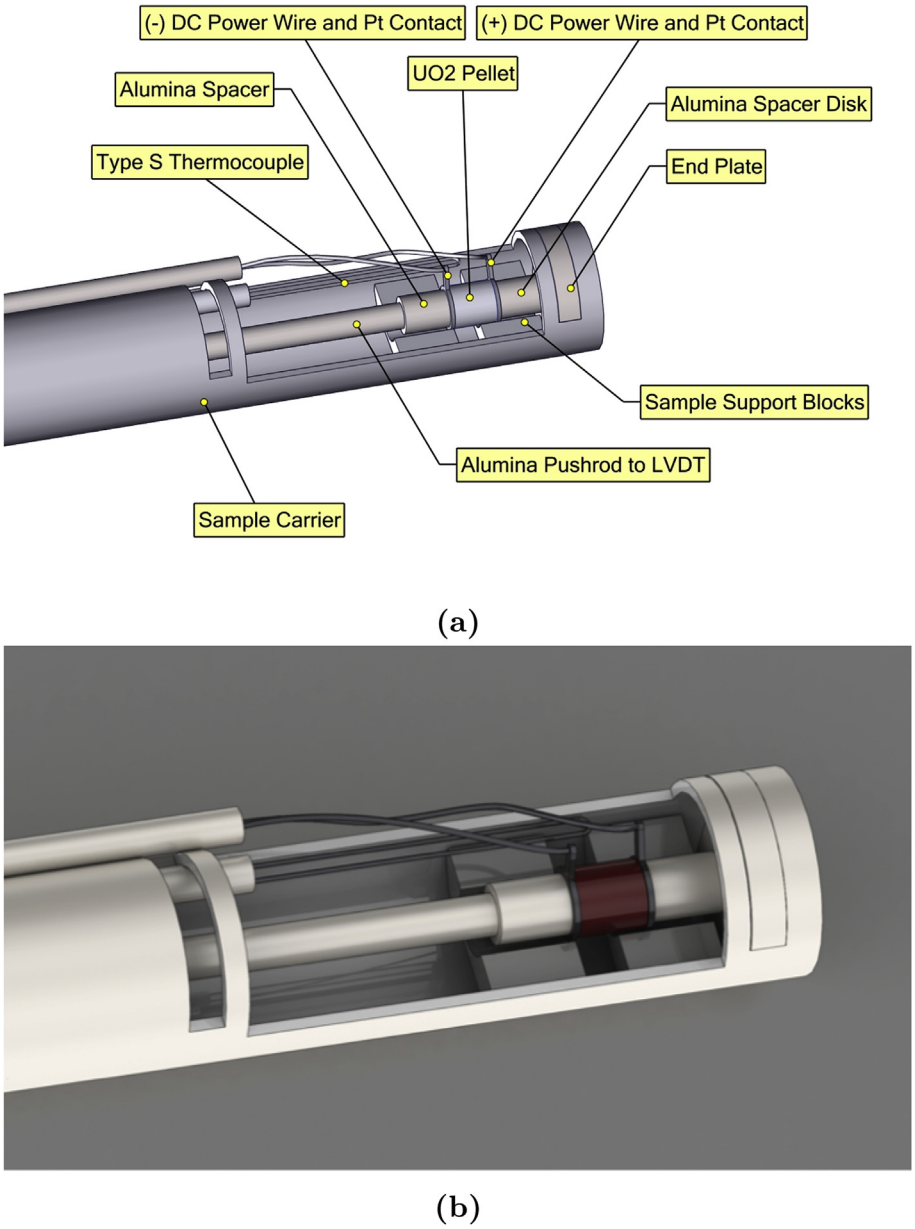

Fig. 1. Schematics showing (a) labeled key components and (b) 3D rendering of flash sintering experiental setup in a Netzsch 402 dilatometer.

The calculated bifurcation diagrams for each composition are plotted in Fig. 5. The heat transfer coefficient h was estimated to be 50 W/m^2 k due to the flowing argon. It is worth noting that for $UO_{2.00}$ at higher temperatures, there is no fold at the surface of the birfucation diagram, indicating that no flash event occurs. Under these circumstances, the current is still increasing due to the exponential decrease in resisitivity, but there is not a sudden jump in temperature characteristic of a flash. This can be recognized as a sort of transition from flash sintering conditions to field enhanced sintering conditions. Unfortuantely, this transition point was not obvious from the experimental data collected, so it has not yet been experimentally verified.

4.1.2. Experiment

The method for determining the critical field at flash was identical for each sample. The furnace was heated to an isothermal temperature and held for 15 min, after which the voltage was ramped at a rate of 1 V/s until a flash occurred. The voltage and current evolution with time was recorded; an example of data collected at room temperature is shown in Fig. 6. During the voltage ramp, the field at which the increase in the current flow became nonlinear was taken as the flash point, where a 5% deviation from linearity was taken as the definition of 'nonlinear.' The lower temperature limit for all samples was room temperature (26°C), but the maximum temperature was dependent upon the magnitude of the field required to flash, which varied with stoichiometry. For instance, it only made sense to test up to 200°C for $UO_{2.08}$, since the critical field was already low at that temperature and the speed at which the flash progressed meant that data collection was limited. The results for the three different stoichiometries are shown in Fig. 7. The graph includes the values determined by the model for comparison, and is therefore missing the model values at higher fields for $UO_{2.00}$ (see Section 4.1.1 for further explanation). The experimental and model results match closely and consistently

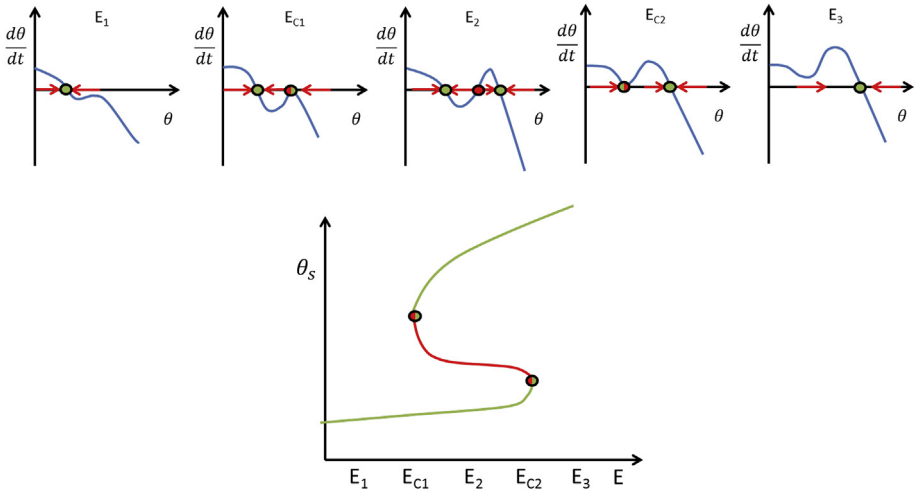

Fig. 2. Flow diagrams and the respective bifurcation diagram.

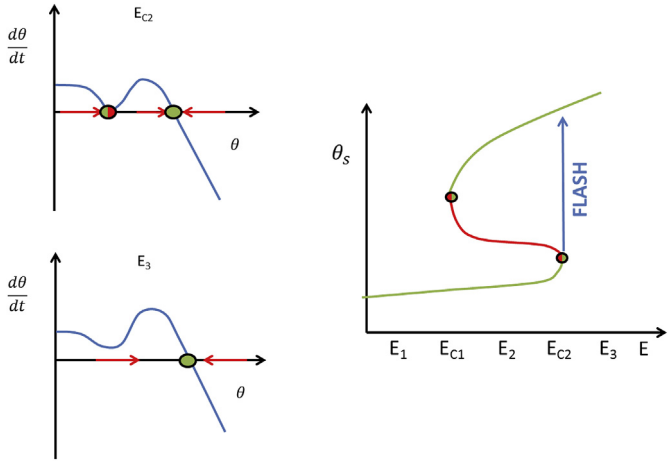

Fig. 3. Thermal runaway on a critical electrical field.

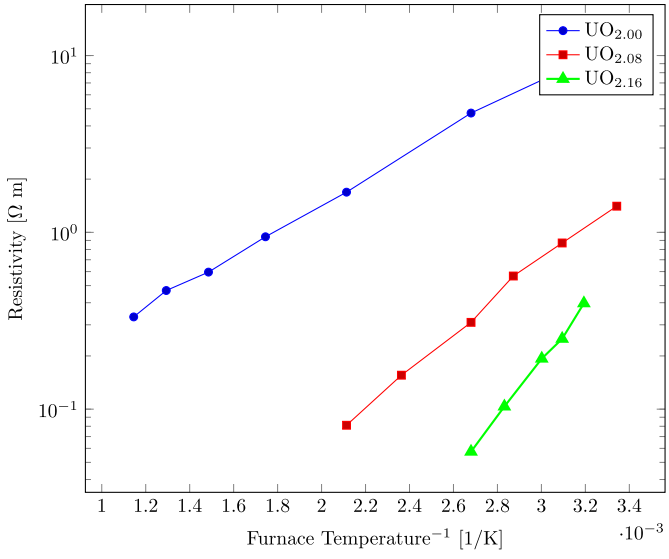

Fig. 4. Arrhenius plot of resistivity as a function of temperature.

Table 1
Measured resistivity parameters for each stoichiometry.

Stoichiometry	$\Omega_0 \cdot [\Omega\ m]$	$\Delta E \cdot [eV]$
$UO_{2.00}$	$5.53 \cdot 10^{-2}$	0.14
$UO_{2.08}$	$5.94 \cdot 10^{-4}$	0.20
$UO_{2.16}$	$3.02 \cdot 10^{-6}$	0.32

show that an increase in oxygen content results in a decrease in the critical field.

4.2. Incubation time

The time required for a flash to occur at room temperature was tested by applying a series of increasing fields to the samples. In these experiments, the field was applied instantly instead of ramped. Data collected during one low field and one high field application on stoichiometric uranium dioxide is shown in Fig. 8. Initially, values around the critical field determined in Section 4.1 were tested. The field was then increased until the flash occurred instantly and subsequently decreased down to a value where a flash would not occur within five minutes. The results are shown in Fig. 9, where the time at which the flash occurred was defined the same as in Section 4.1. This graph shows that for all stoichiometries, the magnitude of the field applied and the time required to flash are inversely related. It also further validates the fact that the increase in sample oxygen content results in a lower field required for flash.

5. Discussion

5.1. Material properties

The results from this study demonstrate that uranium dioxide flashes at temperatures down to room temperature, which is a significantly lower temperature than seen with other materials [25]. One possible explanation lies in the electrical properties of the material. Uranium dioxide is a well-known semiconductor and thermistor, meaning the resistance falls exponentially with an increase in temperature. The heat dissipated by the current passing through the material raises the material temperature, lowering the resistance and increasing the current flow. The increased current

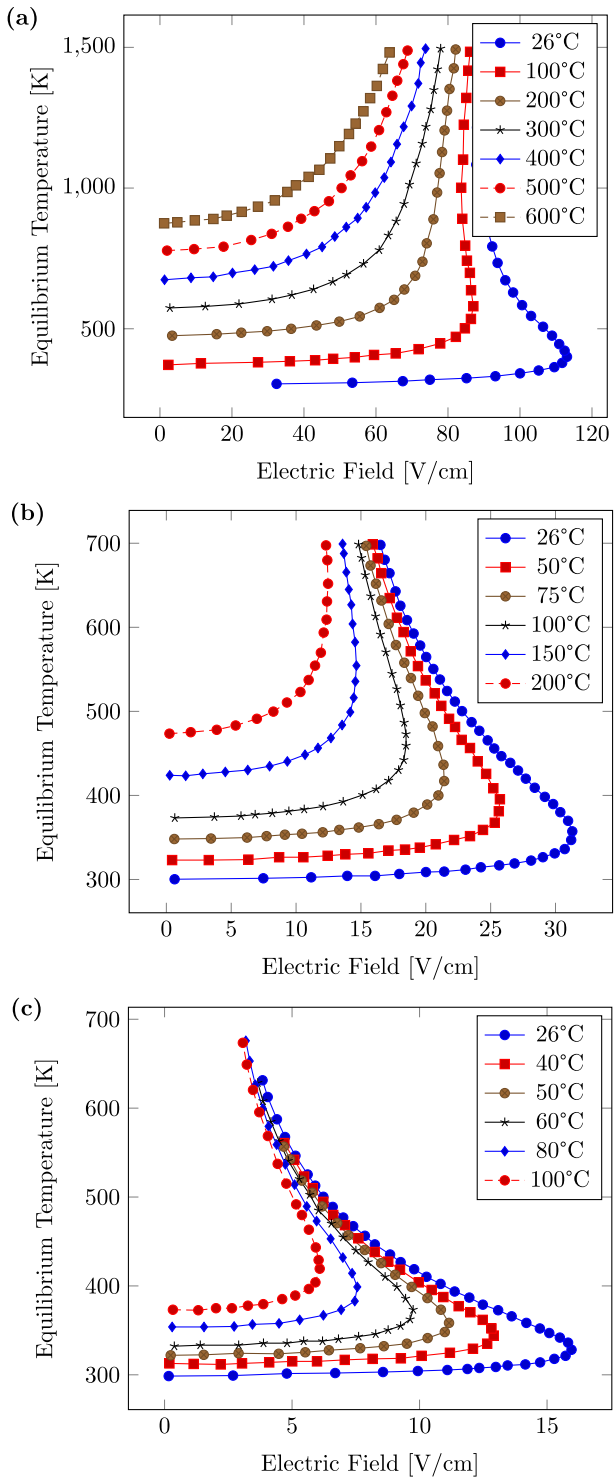

Fig. 5. Bifurcation diagrams for (a) $UO_{2.00}$, (b) $UO_{2.08}$, and (c) $UO_{2.16}$.

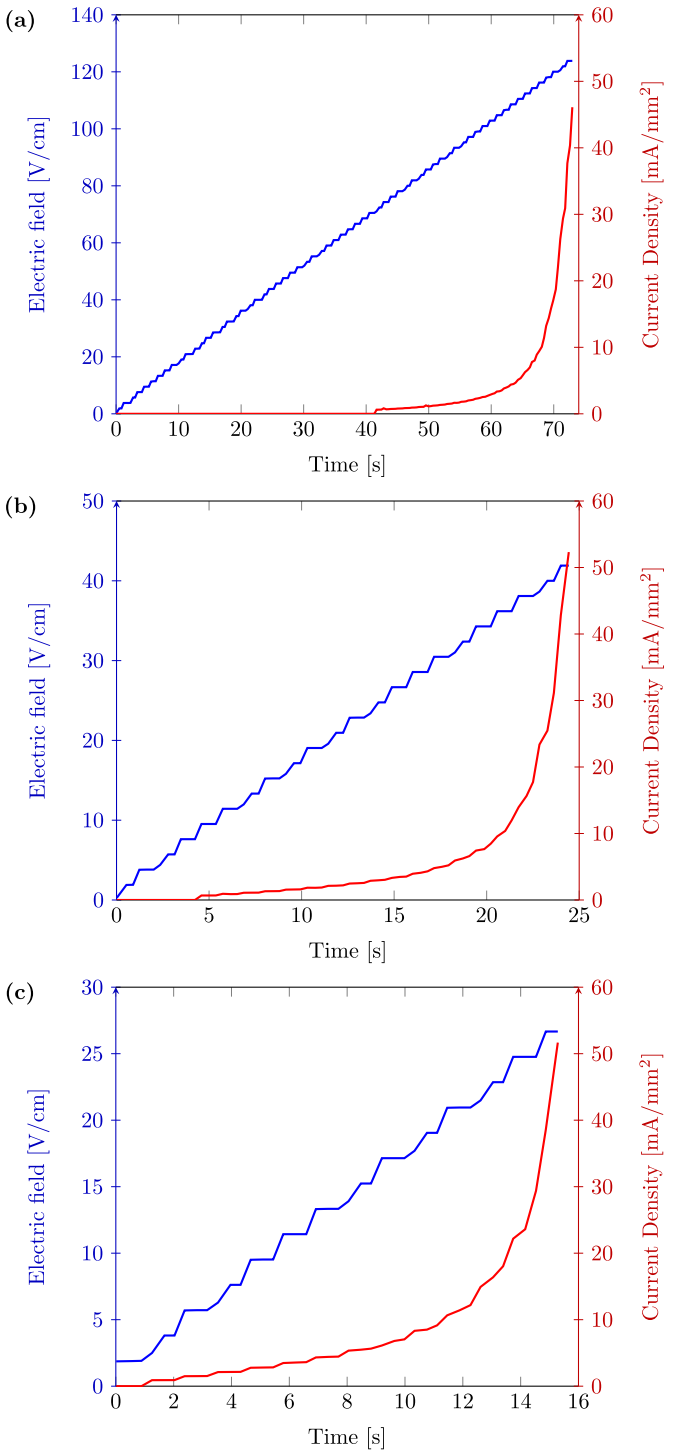

Fig. 6. Experimental parameter profile curves showing the voltage and current evolution at room temperature for (a) $UO_{2.00}$, (b) $UO_{2.08}$ and (c) $UO_{2.16}$. Note that the range for the applied field values is different for each stoichiometry.

flow then causes more heat dissipation, resulting in a thermal runaway positive feedback mechanism. In addition, uranium dioxide has a low thermal conductivity that decreases with increasing temperature up to 1500 °C, after which it slightly increases [31]. The opposing increase in electrical conductivity and decrease in thermal conductivity as the temperature rises in the material may contribute to an enhancement in flash behavior. The onset of densification in conventionally sintered uranium dioxide in an argon atmosphere occurs above 1100°C [26]. Therefore, flash sintering will likely lower the system temperature required to sinter this material.

5.2. Oxygen content

Fig. 7 shows that the field required to flash is reduced by hyperstoichiometry, highlighting the importance of oxygen content on flash sintering behavior. The difference is likely due to the effect of

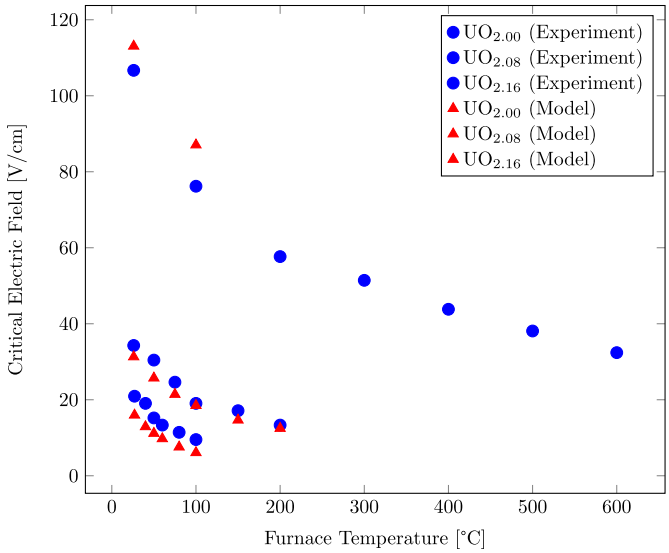

Fig. 7. Comparison of experimentally determined critical field values with those obtained from bifurcation model for $UO_{2.00}$ (blue), $UO_{2.08}$ (red), and $UO_{2.16}$(green). (For interpretation of the references to colour in this figure legend, the reader is referred to the web version of this article.)

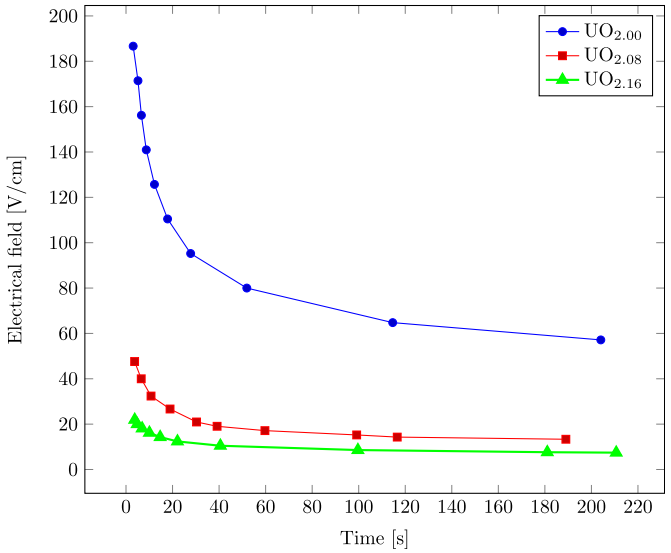

Fig. 9. Plot of the time required to cause a flash under constant applied field at room temperature (26°C) for $UO_{2.00}$ (blue), $UO_{2.08}$ (red), and $UO_{2.16}$ (brown). (For interpretation of the references to colour in this figure legend, the reader is referred to the web version of this article.)

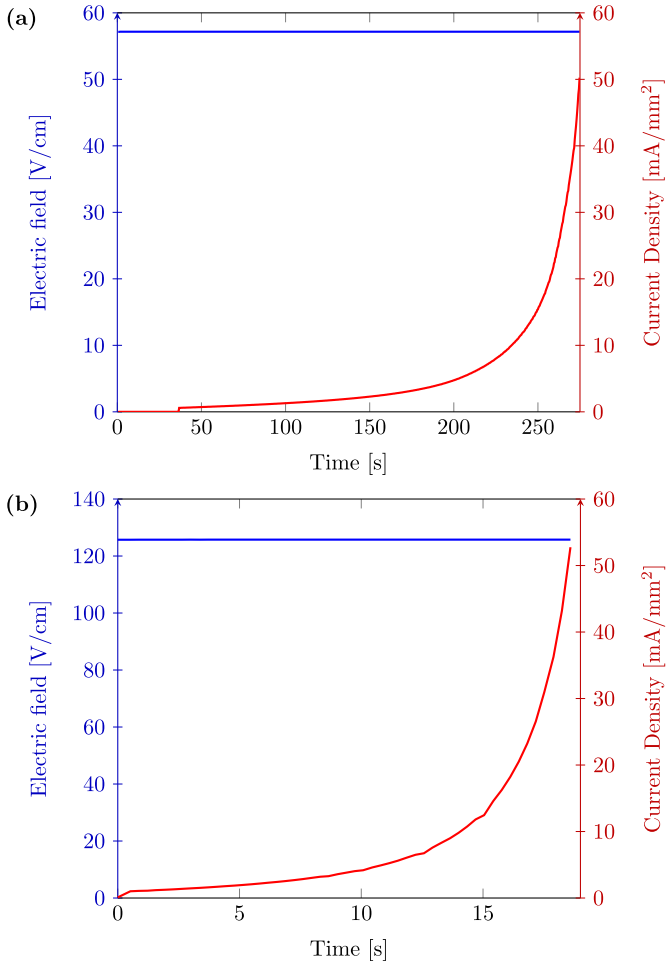

Fig. 8. Experimental parameter profiles for the voltage and current evolution at room temperature for a field of (a) 57 V/cm (incubation time 204 s) and (b) 125 V/cm (incubation time 12 s) applied to $UO_{2.00}$. The results show that a higher applied field results in a lower incubation time.

excess oxygen on the electrical conductivity. Previous work on UO_2 electrical conductivity revealed the material as a positive hole conductor [27]. When excess oxygen is introduced into the lattice, it is accommodated at the interstitial sites of the fluorite structure, forming UO_{2+x}. For each oxygen interstitial, two uranium atoms are oxidized from U^{4+} to U^{5+}. The defective fluorite structure therefore contains U^{4+}, U^{5+}, and oxygen ions. The holes leftover by the higher valence uranium atoms will then move through the material by a polaron hopping mechanism [28,29]. Although the presence of U_4O_9 at lower temperatures will further complicate this mechanism, the trend is still for the electrical conductivity to increase with an increasing O/U composition [30]. In addition, hyper-stoichiometric uranium dioxide has an even lower thermal conductivity in the low temperature range compared to stoichiometric UO_2 [32]. This may contribute to an even further enhancement in sintering. The effect of oxygen content on flash sintering behavior is relevant when considering the starting material properties, since the stoichiometry could potentially be tailored to optimize the fabrication process.

5.3. Experiment vs. model

The experimental results seem to match closely with those given by the model, which further validates the model as reliable for predicting the onset of flash sintering. There could be a number of reasons for the observed differences between the two, including the omission of radiative heat transfer from the model. The model accurately describes the material behavior at low furnace temperatures, which is shown for $UO_{2.00}$ in Fig. 5. The absence of a fold in the bifurcation diagram at high temperatures suggests that the temperature is too high for a traditional flash to occur. In this case, the current will still run through the material and cause it to heat up, but the sudden jump in temperature will not occur. The trend of approaching to this limit at higher temperatures can be seen for all materials in Fig. 5, and it can be understood as a transition from flash sintering to traditional field enhanced sintering. Since this transition point is not obvious from the experimental parameter profiles, coupled modeling may prove to be necessary for determination.

One additional finding from the experiments worth pointing out is that the voltage ramp rate value of 1 V/s has an effect on the critical field, perhaps since there is a time during the ramp where the current is running through the material and causing it to heat up. This is shown experimentally when comparing the results from Section 4.1 with those from Section 4.2. According to Fig. 7, $UO_{2.00}$ should flash at room temperature with an applied field of 107 V/cm, but Fig. 9 shows that it takes a higher field of 187 V/cm when the field is applied instantly. This indicates the existence of effects during the ramp that will lower the apparent field required to flash. These effects have not yet been incorporated into the model.

6. Conclusions

Ongoing flash sintering studies on various materials, like those summarized in this paper, are rapidly contributing to the feasibility of controlling this method for use in the future. This research successfully demonstrates flash sintering of uranium dioxide and contributes some relevant observations on the variability of onset conditions with stoichiometry. The results conclusively show an enhancement in onset flash behavior with an increase in oxygen content, with excess oxygen lowering the field required to flash. The corresponding increase in material electrical conductivity with an increase in oxygen content is proposed as the responsible mechanism. Critical field results from an established bifurcation stability model are consistent with experimental results, further validating the model and verifying the involvement of thermal runaway in the progression of flash sintering. Although these results give information on the effect of oxygen content on the onset conditions for flash, no real conclusions can be made on the effect on densification. Therefore, densification studies are being completed in order to determine how separate parameters influence sinterability of uranium dioxide using flash sintering.

Acknowledgements

This work was supported by the U.S. Department of Energy Office of Nuclear Energy's Fuel Cycle Research and Development (FCRD) program. Work at Los Alamos National Laboratory was performed under the auspices of the U.S. Department of Energy (contract no. DE-AC52-06NA25396).

References

[1] V. Yemelyanox, A. Yevstyukhim, The Metallurgy of Nuclear Fuel, Pergamon Press, London, 1969.
[2] OECD Nuclear Energy Agency, Uranium 2014 : Resources, Production and Demand, 2014, p. 488.
[3] N. Fuhrman, L. Hower, R. Holden, Low temperature sintering of uranium dioxide, J. Am. Ceram. Soc. (1963) 114–121.
[4] X.-d. Yang, J.-c. Gao, Y. Wang, X. Chang, Low-temperature sintering process for UO_2 pellets in partially-oxidative atmosphere, Trans. Nonferrous Metals Soc. China (English Ed. 18 (1) (2008) 171–177.
[5] Z.A. Munir, U. Anselmi-Tamburini, M. Ohyanagi, The effect of electric field and pressure on the synthesis and consolidation of materials: a review of the spark plasma sintering method, J. Mater. Sci. 41 (3) (2006) 763–777.
[6] O. Guillon, J. Gonzalez-Julian, B. Dargatz, T. Kessel, G. Schieming, J. Ratehl, M. Hermann, Field assisted sintering technology/spark plasma sintering: mechanisms, materials, and technology developments, Adv. Eng. Mater. (2014), http://dx.doi.org/10.1002/adem.201300409.
[7] L. Ge, G. Subhash, R.H. Baney, J.S. Tulenko, E. McKenna, Densification of uranium dioxide fuel pellets prepared by spark plasma sintering (SPS), J. Nucl. Mater. 435 (1–3) (2013) 1–9.
[8] J.H. Yang, K.W. Song, Y.W. Lee, J.H. Kim, K.W. Kang, K.S. Kim, Y.H. Jung, Microwave process for sintering of uranium dioxide, J. Nucl. Mater. 325 (2–3) (2004) 210–216.
[9] S. Yeo, E. McKenna, R. Baney, G. Subhash, J. Tulenko, Enhanced thermal conductivity of uranium dioxide-silicon carbide composite fuel pellets prepared by Spark Plasma Sintering (SPS), J. Nucl. Mater. 433 (1–3) (2013) 66–73.
[10] K.D. Johnson, A.M. Raftery, D.A. Lopes, J. Wallenius, Fabrication and microstructural analysis of UN-U_3 Si_2 composites for accident tolerant fuel applications, J. Nucl. Mater. 477 (2016) 18–23.
[11] M. Cologna, B. Rashkova, R. Raj, Flash sintering of nanograin zirconia in <5 s at 850°C, J. Am. Ceram. Soc. 93 (11) (2010) 3556–3559.
[12] E. Bichaud, J.M. Rashkova, C. Carry, M. Kleitz, M.C. Steil, Flash sintering incubation in Ali_2 Oi_3/TZP composites, J. Eur. Ceram. Soc. 35 (2015) 2587–2592.
[13] A. Gaur, V.M. Sglavo, Flash-sintering of MnCo2O4 and its relation to phase stability, J. Eur. Ceram. Soc. 34 (10) (2014) 2391–2400.
[14] H. Yoshida, Y. Sakka, T. Yamamoto, J.M. Lebrun, R. Raj, Densification behaviour and microstructural development in undoped yttria prepared by flash-sintering, J. Eur. Ceram. Soc. 34 (4) (2014) 991–1000.
[15] E. Zapata-Solvas, S. Bonilla, P.R. Wilshaw, R.I. Todd, Preliminary investigation of flash sintering of SiC, J. Eur. Ceram. Soc. 33 (13–14) (2013) 2811–2816.
[16] J.A. Downs, V.M. Sglavo, Electric field assisted sintering of cubic zirconia at 390°C, J. Am. Ceram. Soc. 96 (5) (2013) 1342–1344.
[17] J.S.C. Francis, R. Raj, Influence of the field and the current limit on flash sintering at isothermal furnace temperatures, J. Am. Ceram. Soc. 96 (9) (2013) 2754–2758.
[18] H. Yoshida, K. Morita, B.N. Kim, Y. Sakka, T. Yamamoto, Reduction in sintering temperature for flash-sintering of yttria by nickel cation-doping, Acta Mater. 106 (2016) 344–352.
[19] J.E. Garay, S.C. Glade, U. Anselmi-Tamburini, P. Asoka-Kumar, Z.A. Munir, Electric current enhanced defect mobility in Ni^3 Ti intermetallics, Appl. Phys. Lett. 85 (4) (2004) 573–575.
[20] C.S. Bonifacio, T.B. Holland, K. Van Benthem, Evidence of surface cleaning during electric field assisted sintering, Scr. Mater. 69 (11–12) (2013) 769–772.
[21] R. Baraki, S. Schwarz, O. Guillon, Effect of electrical field/current on sintering of fully stabilized zirconia, J. Am. Ceram. Soc. 95 (1) (2012) 75–78.
[22] J.G.P. da Silva, H.A. Al-Qureshi, F. Keil, R. Janssen, A dynamic bifurcation criterion for thermal runaway during the flash sintering of ceramics, J. Eur. Ceram. Soc. 36 (5) (2016) 1261–1267.
[23] Y. Dong, I.W. Chen, Onset criterion for flash sintering, J. Am. Ceram. Soc. 98 (12) (2015) 3624–3627.
[24] R.I. Todd, E. Zapata-Solvas, R.S. Bonilla, T. Sneddon, P.R. Wilshaw, Electrical characteristics of flash sintering: thermal runaway of Joule heating, J. Eur. Ceram. Soc. 35 (6) (2015) 1865–1877.
[25] R. Raj, On the Power Density at the Onset of Non-linearity in Experiments Related to Flash Sintering, vol. 7, 2015, pp. 1–7.
[26] T.R.G. Kutty, P.V. Hegde, K.B. Khan, U. Basak, S.N. Pillai, A.K. Sengupta, G.C. Jain, S. Majumdar, H.S. Kamath, D.S.C. Purushotham, Densification behaviour of UO_2 in six different atmospheres, J. Nucl. Mater. 305 (2–3) (2002) 159–168.
[27] W. Hartmann, Ziet. Phys. 102 (1936) 709.
[28] G. Casado, J.M. Harding, J.H. Hyland, Small-polaron hopping in mott-insulating UO_2, J. Phys. Condens. Matter 6 (1944) 4685–4698.
[29] T. Ishii, K. Naito, K. Oshima, Electrical conductivity and defect structures in non-stoichiometric UO_{2+x}, J. Nucl. Mater. 36 (1970) 288–296.
[30] H. Lee, Electrical conductivity of UO_{2+x}, J. Nucl. Mater. 50 (1974) 25–30.
[31] A.D. Feith, Thermal Conductivity of UO_2 by Radial Heat Flow Method, 1963. TM-63-9-5.
[32] J. White, A. Nelson, Thermal conductivity of UO_{2+x} and U_4 O_{9-y}, J. Nucl. Mater. 443 (2013) 342–350.